crystals

MDPI

Article

Bio-Mediated Method for Immobilizing Copper Tailings Sand Contaminated with Multiple Heavy Metals

Bo Kang [1], Fusheng Zha [1,*], Hongchang Li [1,2], Long Xu [1], Xianguo Sun [3] and Zhitang Lu [1]

[1] School of Resource and Environmental Engineering, Hefei University of Technology, Hefei 230009, China; kangbo@hfut.edu.cn (B.K.); ywlihongchang@163.com (H.L.); xulong_2005@hfut.edu.cn (L.X.); zhitang_lu@163.com (Z.L.)
[2] Energy Exploration Center, Geological Exploration Technology Institute of Anhui Province, Hefei 230031, China
[3] Anhui Huizi Construction Engineering Co., Ltd., Wuhu 241004, China; ss8211050302@163.com
* Correspondence: geozha@hfut.edu.cn; Tel.: +86-136-9653-3099

Abstract: Microbial induced carbonate precipitation (MICP) is a natural bio-mediated process that has been investigated for soil stabilization and heavy metal immobilization in soil and groundwater. This study analyzed the effect and mechanism of MICP for the solidification/stabilization of tailings sand with multi-heavy metals. When the concentration of cementation solution (CS) is 1.0 mol/L and the optical density(OD_{600}) is 1.6, the unconfined compressive strength of tailings sand treated by MICP is the largest, and the solidification efficiency of heavy metals in tailings sand is also the highest. The macroscopic and microscopic observations reveal that the mechanism of MICP solidification of tailings is bacterial outer oxide, hydroxide, alkaline carbonate, and carbonate precipitation.

Keywords: microbial induced carbonate precipitation; *Sporosarcina pasteurii*; copper tailings sand; multi-heavy metals

check for updates

Citation: Kang, B.; Zha, F.; Li, H.; Xu, L.; Sun, X.; Lu, Z. Bio-Mediated Method for Immobilizing Copper Tailings Sand Contaminated with Multiple Heavy Metals. *Crystals* **2022**, *12*, 522. https://doi.org/10.3390/cryst12040522

Academic Editors: Hamed Khodadadi Tirkolaei, Satoru Kawasaki, Liang Cheng, Leon van Paassen and Claudia Graiff

Received: 25 February 2022
Accepted: 6 April 2022
Published: 8 April 2022

Publisher's Note: MDPI stays neutral with regard to jurisdictional claims in published maps and institutional affiliations.

Copyright: © 2022 by the authors. Licensee MDPI, Basel, Switzerland. This article is an open access article distributed under the terms and conditions of the Creative Commons Attribution (CC BY) license (https://creativecommons.org/licenses/by/4.0/).

1. Introduction

Copper tailings are powdery or sandy solid wastes produced by copper ore beneficiation. According to the analysis report of China's solid waste treatment industry in 2021, the annual emission of copper tailings slag in China can reach 335 million tons. Immense quantities of tailings accumulate in the form of large hills or water ponds, which may cause severe problems. Sometimes, large tailing dumps are unstable and suffer from slope instability effecting by water content changes, which may cause geo-hazards such as landslides. Furthermore, as reservoirs of heavy metal-containing wastes such as Cu, Pb, Zn, Cd, and Cr, copper mine tailings pose significantly substantial risk to the ecosystem and human health due to their toxicity [1,2]. Small particles of tailings may be carried by wind to nearby communities and cause air pollution. Water and soil pollution may occur when rain falls on the tailings and leaches the metals [3]. Therefore, it is of great importance to find low energy consumption, fast, efficient, and environmentally friendly way to manage these tailings and reduce risks.

Microbial induced carbonate precipitation (MICP) has been proven to be economical, effective, and environmentally friendly [4–8]. One of the most widely adopted pathways to achieve MICP is hydrolysis of urea by urease enzyme, which has the advantages of low cost, high efficiency in triggering cementation, controllable reaction process, and straightforward isolation and harvest process [9]. Among them, *Sporosarcina pasteurii* is the most effective urease-producing bacterial species. The fundamental principle of MICP is that urease-producing bacteria are able to produce urease to decompose urea into ammonium (NH_4^+) and carbonate (CO_3^{2-}), then NH_4^+ releases ammonia (NH_3) and increases the pH value of the medium until NH_4^+/NH_3 and HCO_3^-/CO_3^{2-} reach a balance. After these reactions, the pH is close to 9.3 whereby $CaCO_3$ precipitation occurs via a combination of Ca^{2+} and

CO_3^{2-} [10]. The precipitated $CaCO_3$ fills the soil pores and cements the soil particles, which improves the soil strength and reduces the permeability. Meanwhile, the heavy metal ions are co-precipitated and immobilized, which can significantly reduce the concentration of exchangeable heavy metal ions.

In the MICP process, by replacing the calcium with other divalent elements, strong absorption of heavy metals on the surface and inside the lattice of calcite occurs [11]. However, more than five million contaminated sites have been reported globally, in particular mine tailing sites, covering 20 million hectares of land, in which the soils are contaminated by the heavy metals, such as Cu, Pb, Cd, As, Cr, Co, Hg, Ni, Zn, and Se, and which have soil concentrations above background values or regulatory levels [12–17]. The effect and mechanism of ureolytic-driven MICP for immobilizing multi-heavy-metal contaminated soils has not been explained clearly. This mechanism can be crucial in applications, as polluted soil like tailing sand invariably contains multiple metal elements, which may have a significant impact on the effect of immobilization. The presence of heavy metals in the soil will undoubtedly affect the curing efficiency of microorganisms.

Using MICP (including the ureolytic-driven MICP) method, this study chooses tailings sand polluted by various heavy metals for study, and explores the followings: (1) the unconfirmed compressive strength (UCS) and durability of tailings sand under different concentrations; (2) the removal rate of different ions; and (3) the microstructure of solidified tailings sand by XRD and SEM. The solidification mechanism and the hypothesis of multi-layer precipitation structure by MICP of various heavy metals is proposed for the first time in this study.

2. Materials and Testing Methods

2.1. Bacteria and Chemicals

Sporosarcina pasteurii (*S. pasteurii*, ATCC 6452), a non-pathogenic bacterium with high urease activity, was used in this study for MICP [18,19]. The bacterial solution was prepared by inoculating bacterial colonies into the NH_4-YE solution medium (20 g/L yeast extract, 10 g/L $(NH_4)_2SO_4$, and 0.13 M Tris-base) and was then subjected to shaking incubation at 30 °C for approximately 24 h until the optical density at 600 nm (OD_{600}) reached the designated value. The OD_{600} value was measured via a UV-Visible spectrometer (Shanghai Analytical Instruments Co Ltd., Shanghai, China). The prepared bacterial solution was then stored at 4 °C. Prior to its use in the experiment, it was firstly re-harvested in fresh growth medium. When bacteria cells reached the exponential growth stage during resuscitation, they were inoculated into the solution for the formal test. NH_4-YE medium, $CaCl_2$, and urea solutions were sterilized by autoclaving at 121 °C for 20 min.

The actual number of cells can be converted by Equation (1) [20].

$$Y = 8.59 \times 10^7 Z^{1.3627} \quad (1)$$

where Y was cell concentration (cells ML^{-1}) and Z is OD_{600}

2.2. Tailings Sand

Copper mine tailing samples were collected from the Shuimucong tailing pond (117°51′2″ E, 30°55′42″ N), which is located in Tongling city, a typical mining city in Southeast China. According to the test results, the average particle size (D_{50}) was 0.28 mm, the nonuniformity coefficient (C_u) was 4.62, and the curvature coefficient (C_C) was 1.58. The tailings were medium-fine sand with poor grading and uniform distribution. The natural moisture content was 9.46%, while the loose bulk density was 1.32 g/cm^3, and the specific gravity was 2.86. Some physicochemical properties and the background levels of toxic metals in the soil are shown in Table 1.

Table 1. Chemical properties of mine tailing soil.

XRF	Mass Fraction (%)	Element	Mass per Kilogram (g)	Mass Fraction Ratio (%)
SiO_2	66.82	Si	311.8416	57.83
Al_2O_3	13.42	Al	71.0846	13.18
CaO	8.88	Ca	79.3259	14.71
Fe_2O_3	3.71	Fe	26.0029	4.82
K_2O	3.07	K	25.4877	4.73
MgO	1.90	Mg	11.4462	2.12
Na_2O	0.90	Na	6.7078	1.24
TiO_2	0.62	Ti	3.7470	0.69
P_2O_5	0.25	P	1.1265	0.21
SO_3	0.13	S	0.5432	0.10
MnO	0.06	Mn	0.5051	0.09
ZrO_2	0.05	Zr	0.4372	0.08
SrO	0.04	Sr	0.3901	0.07
Cr_2O_3	0.04	Cr	0.3102	0.06
Rb_2O	0.01	Rb	0.1700	0.03
ZnO	0.01	Zn	0.0690	0.01
NiO	0.01	Ni	0.0503	0.01

The XRF results showed that the tailings contained more Al and Ca compounds. The results of the electron microprobe show that it contains dolomite, potassium feldspar, plagioclase, muscovite, clinopyroxene, garnet, and pyrite. The heavy metal elements in the tailings sand were determined by the toxicity characteristic leaching procedure (TCLP), and the calcium carbonate content was measured according to the excessive acid dissolution method (other carbonates are converted to calcium carbonate). The results showed that Cu, Zn, Mn, and Pb significantly exceeded the standard (GB36600-2018). As shown in Table 1 by X-ray fluorescence spectrosecopy (XRF) technique to determine the chemical oxides in the soil are mainly silica, aluminum oxide, calcium oxide, iron trioxide, etc. The results of the electron microprobe show that it contains dolomite, potassium feldspar, plagioclase, muscovite, clinopyroxene, dolomite, garnet, and pyrite. The heavy metal elements in the tailings sand were determined by the toxicity characteristic leaching procedure (TCLP), and the calcium carbonate content was measured according to the excessive acid dissolution method (other carbonates are converted to calcium carbonate). The results showed that Cu, Zn, Mn, and Pb significantly exceeded the standard (GB36600-2018).

2.3. Sample Concentration

The objective of the mine tailing immobilization test was to determine the heavy metal immobilization efficiency via MICP at different initial bacterial concentrations and calcium sources. Three experimental settings were designed to examine the effects of calcium source and initial bacteria concentration on Cu, Zn, Mn, and Pb the immobilization efficiency via MICP. The test scheme and sample label is shown in Table 2. The concentration of bacteria was chosen as OD_{600} = 0.8, 1.0, 1.2, 1.4, and 1.6, and the concentration of the cementation solution (CS) was 0.5 (Group A), 1.0 (Group B) and 1.5 (Group C) mol/L, respectively. The step-by-step grouting method was used, and the bacterial liquid or cementitious liquid was slowly injected into the sample by a peristaltic pump eight times (Figure 1). The steps of injections are as follows:(a) 50 mL bacterial suspension was injected from the top to bottom with an inflow rate of about 2 mL/min; (b) 5 mL fixation solution was flushed with the same inflow rate as the bacterial suspension; and (c) 400 mL CS was injected from the top to bottom with an inflow rate of about 0.2 mL/min.

Table 2. Test scheme and sample label.

Concentration of CS (mol/L) \ OD_{600}	0.8	1.0	1.2	1.4	1.6
0.5	A1	A2	A3	A4	A5
1.0	B1	B2	B3	B4	B5
1.5	C1	C2	C3	C4	C5

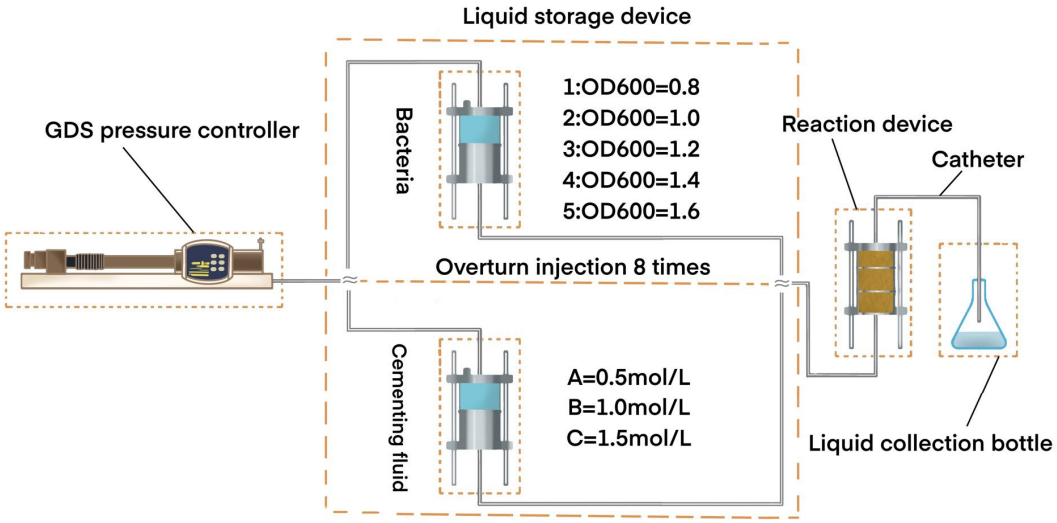


Figure 1. Schematic drawing of the testing procedure.

2.4. Methods

(1) UCS test

In accordance with the standard test method for UCS of the immobilization mine tailings (ASTM D2166/D2166M-16 2016), the as-prepared specimen was assembled in a strain-controlled YHS-2 UCS testing apparatus. The UCS test was then performed at a vertical strain rate of 1%/min. The stress and strain of the specimen were recorded at intervals of 5 s until the specimen failed.

(2) Leaching experiment of simulated atmospheric rainfall

To measure the immobilization rate of different ions in tailings, this study verified the heavy metal leaching of samples under atmospheric rainfall. A set of self-made devices was used to simulate the rainfall leaching test [21]. The leachates were collected, and the heavy metal content was measured by atomic absorption spectrometry. Then the removal rate of heavy metal can be calculated by Equation (2).

$$Removal\ rate = 1 - \frac{C_m}{C_0} \quad (2)$$

where C_m is the leaching concentration of heavy metals after solidification and C_0 is the leaching concentration of heavy metals in the unsolidified sample.

(3) XRD and SEM analysis

The control and treated soil samples were analyzed by XRD (Hefei, China) and SEM (Hefei, China) to confirm metal bioimmobilization. XRD patterns were obtained using a Rigaku D/Max-2005 V diffractometer with Cu-Kα scanning from 5 to 80°2θ. After natural drying, the samples were crushed and ground using a mortar and pestle before being

mounted on a glass filter using a tubular aerosol suspension chamber. The components in the samples were identified by comparing them with standards established by the International Center for Diffraction Data.

3. Results

3.1. Results and Analysis of Unconfined Test

3.1.1. Strength

It can be seen from Figure 2a that the tailings solidified by all concentrations of bacteria and CS exhibited unconfined compressive strength enhancement. The UCS of all groups was improved in different rate with the increasing of bacterial concentration and CS. With the increase in bacterial concentration, the curing effect of each group was improved, especially in group B, where the UCS was 778 kPa at high bacterial concentration (OD600 = 1.6). The UCS increasing rate of group B was the highest at high bacterial concentration, which was much higher than that of groups A and C at the same bacterial concentration. As the CS content provided by group A was relatively low, increasing the bacterial concentration did not significantly improve the curing effect. The high concentration of CS in group C could inhibit bacteria growth. The increasing rate of UCS of the three groups showed a trend of "fast followed by slow" with the increase of bacterial concentration, which demonstrated that the effect of increasing bacterial concentration on improving the curing effect was significant at low CS concentrations, and gradually decreased at high concentrations. Therefore, the curing effect of group B was better than that of groups A and C at high bacterial concentrations. The unconfined compressive strength of the column sample of biocured tailings obtained in this test is 238 kpa higher than that of the sample made by Oliveira et al. (2021) [22].

3.1.2. Calcium Carbonate Content

The output of the carbonate in tailings after solidification was used to measure the strength effect of solidification.

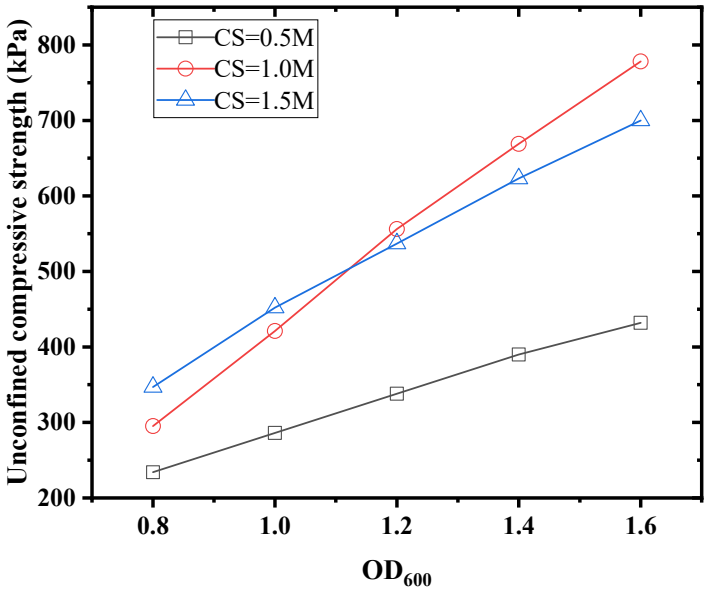
$$W(\%) = \frac{M_1 - M_2}{M_1} \times 100\% \quad (3)$$

where M_1 and M_2 are the qualities of the sand sample before and after the hydrochloric acid reaction, respectively. The carbonate contents of the tailings sand solidified by different bacterial concentrations and CS are shown in Figure 2b.

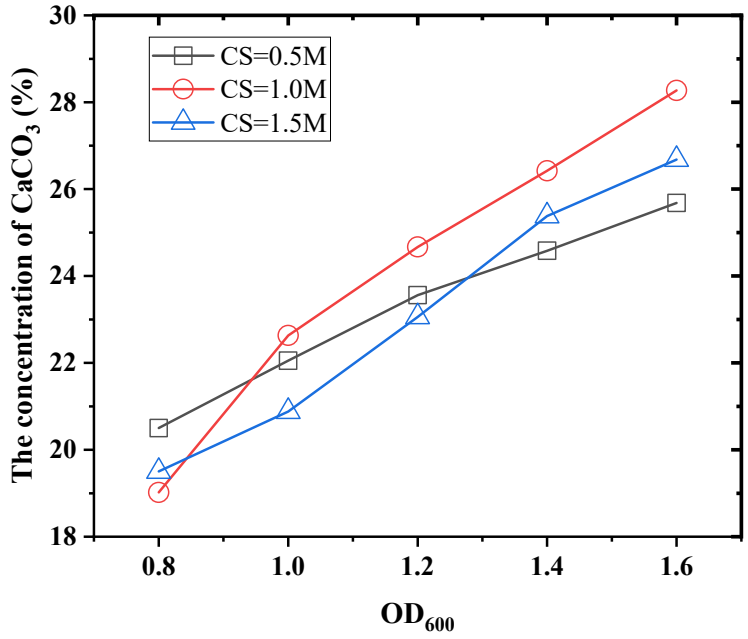
As can be seen from Figure 2b, the content of calcium carbonate is positively correlated with the concentration of bacterial. When the bacterial concentration was low (OD600 = 0.8), the calcium carbonate content was 18.48–20.5%, and the calcium carbonate increment was between 2.66% and 4.68%. At high bacterial concentration (OD600 = 1.6), the calcium carbonate content reached 23.16–27.27%, and the increment of calcium carbonate reached 7.34–11.45%. With the increase in bacterial concentration, the calcium carbonate content increased gradually, showing first fast and then slow trend. The calcium carbonate content of three groups indicated that CS concentration 1 M was the optimal concentration for solidifying copper tailings. The produced rate of calcium carbonate in groups A and C was slower than that in group B.

3.2. Leaching Characteristics

The leaching concentration of heavy metals after solidification of tailings sand is an important index for the evaluation of solidification effect. This test compares the variation characteristics of copper, lead, zinc, and manganese in tailings before and after solidification.



(**a**)



(**b**)

Figure 2. Test results of UCS and $CaCO_3$ concentration. (**a**) Unconfined Compressive Strength; (**b**) $CaCO_3$ Concentration.

3.2.1. Copper

The results in Figure 3a illustrated that the solidification effect of Cu was remarkable, and a higher bacterial concentration may promote Cu precipitation. The highest removal rate of copper ion can reach 99.6%. Specifically, when the bacterial concentration increased from 0.8 to 1.0, the solidification curve had a maximal slope. When the bacterial concentration OD_{600} was 0.8, the solidification effect of group A (0.5 M) was better than that of group B (1.0 M) and group C (1.5 M). With the increase in bacterial concentration, the leaching concentration of Cu in groups A and B was close to 0 mg/kg, while the effect of group C was higher than 0.5 mg/kg.

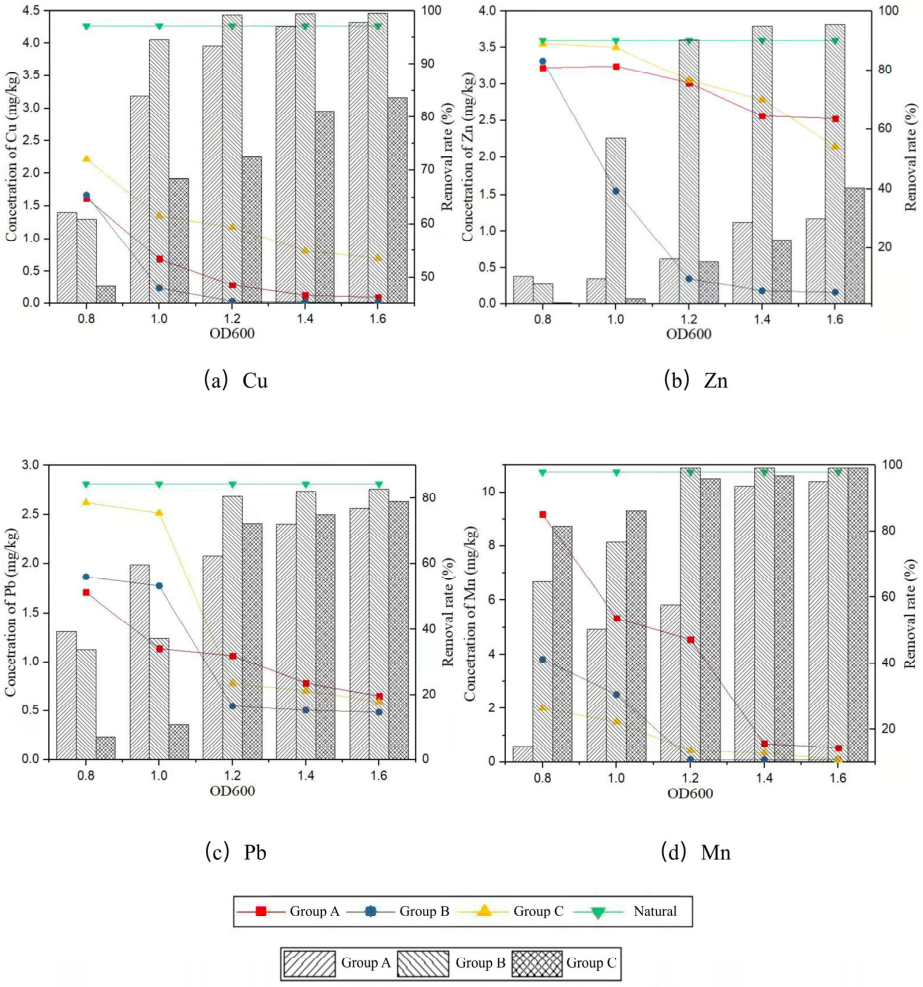


Figure 3. The solidification results of (**a**) Cu, (**b**) Zn, (**c**) Pb, (**d**) Mn under different bacterial concentration.

3.2.2. Zinc

It can be seen from Figure 3b that the curing efficiency of zinc ions varies greatly under the conditions of different bacterial solution concentrations and different cement solution concentrations. The highest curing efficiency of group A and group C was 29.8% and 40.4%, while that of group B was 95.6%. Previously, the curing efficiency using the same strain was only 68.86% [11].

3.2.3. Manganese

As Figure 3c shows, when the concentration of bacterial solution was 0.8, the curing efficiency of manganese ion in group A was only 14.7%, while that in group C was 81.5%. When the concentration of bacterial solution increased, the solidification efficiency of manganese ion in group B increased the fastest. When the bacterial concentration was relatively high (OD_{600} > 1.4), the manganese ion solidification effect of all three groups showed good efficacy. The amount of urea and Ca^{2+} provided by 0.5 mol/L was slight, and the coprecipitation effect was weak, so the curing effect was poor. However, high concentration of 1.5 mol/L CS can inhibit bacteria, and the curing effect is not as effective as 1.0 mol/L.

3.2.4. Lead

The concentration of Pb^{2+} in group C (1.5 M) was essentially the same as that of the control group at low bacterial concentration (OD_{600} = 0.8), while the concentration of Pb^{2+} of group A (0.5 M) and group B (1.0 M) was significantly lower, indicating that Pb had a certain solidification effect when the bacteria concentration was low and the CS

concentration was not excessively high. With the increase in the bacterial concentration, the curing effect improved, especially in group C. At high bacterial concentration (OD_{600} = 1.6), the concentration of Pb^{2+} of groups A, B, and C was at the same level, indicating that the effect of the Pb^{2+} concentration was significantly reduced at high bacterial concentrations.

Three possible reasons were deduced. First, when the concentration of the bacteria was low, the CO_3^{2-} produced by urease decomposing urea was also low. Therefore, the coprecipitation and adsorption effects were weak, making solidification unsatisfactory. When the concentration was high, the reverse applied. Second, when the bacterial concentration was low, the amount of vaterite produced was also lower. A small amount of vaterite cannot adsorb more Mn^{2+}, therefore, increasing the bacterial concentration can increase the production of $CaCO_3$, so the removal rate of Mn^{2+} obviously improved. Third, the concentration of the CS mainly affects the content of urea and Ca^{2+}.

3.3. Microcosmic Mechanism of Tailings Solidified by MICP

3.3.1. XRD Results

The solidified sample was dried and ground into a powder, and then put into the shl-2 X-ray diffractometer instrument for XRD testing. Three groups of samples were marked as A5, B5 and C5, and the original tailings were denoted as A0.

The wave peaks of A5, B5, and C5 among the original tailings and the solidified tailings are shown in Figure 4, which indicates that new minerals and compounds were formed in the tailings by MICP. Aragonite was found in both A5 and C5, where there was no vaterite in the undisturbed tailings. This proved that vaterite was a newly formed mineral of MICP. Comparing the XRD results of undisturbed tailings with the solidified tailings, it was found that vaterite, zinc carbonate, lead carbonate, manganese dioxide, and basic copper carbonate are newly formed in tailings during the MICP process. These results illustrate that MICP produces calcium carbonate precipitation and precipitates Cu, Zn, Mn, Pb, and other heavy metals.

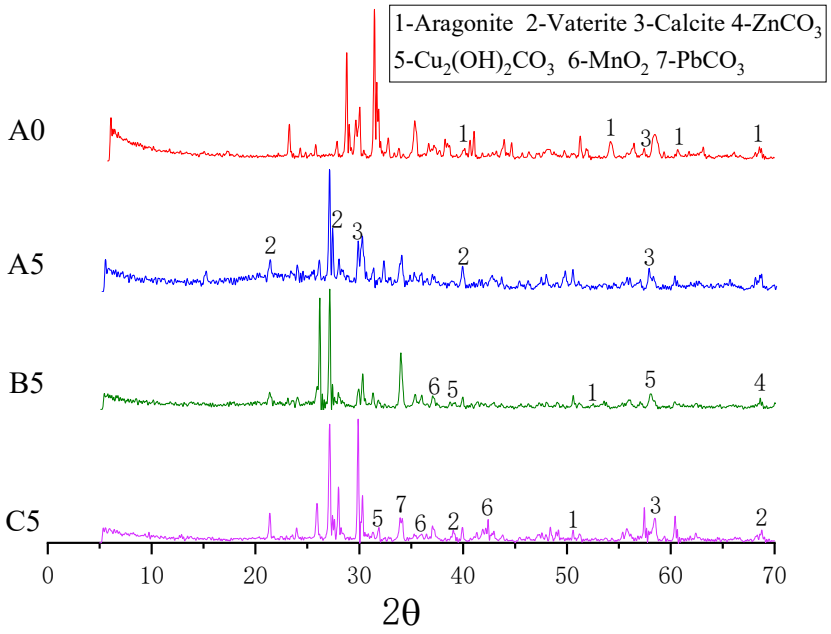


Figure 4. XRD results of A0, A5, B5, and C5.

3.3.2. SEM Results

The SEM results of the A5, B5, and C5 of the tailings after solidification are shown in Figure 5.

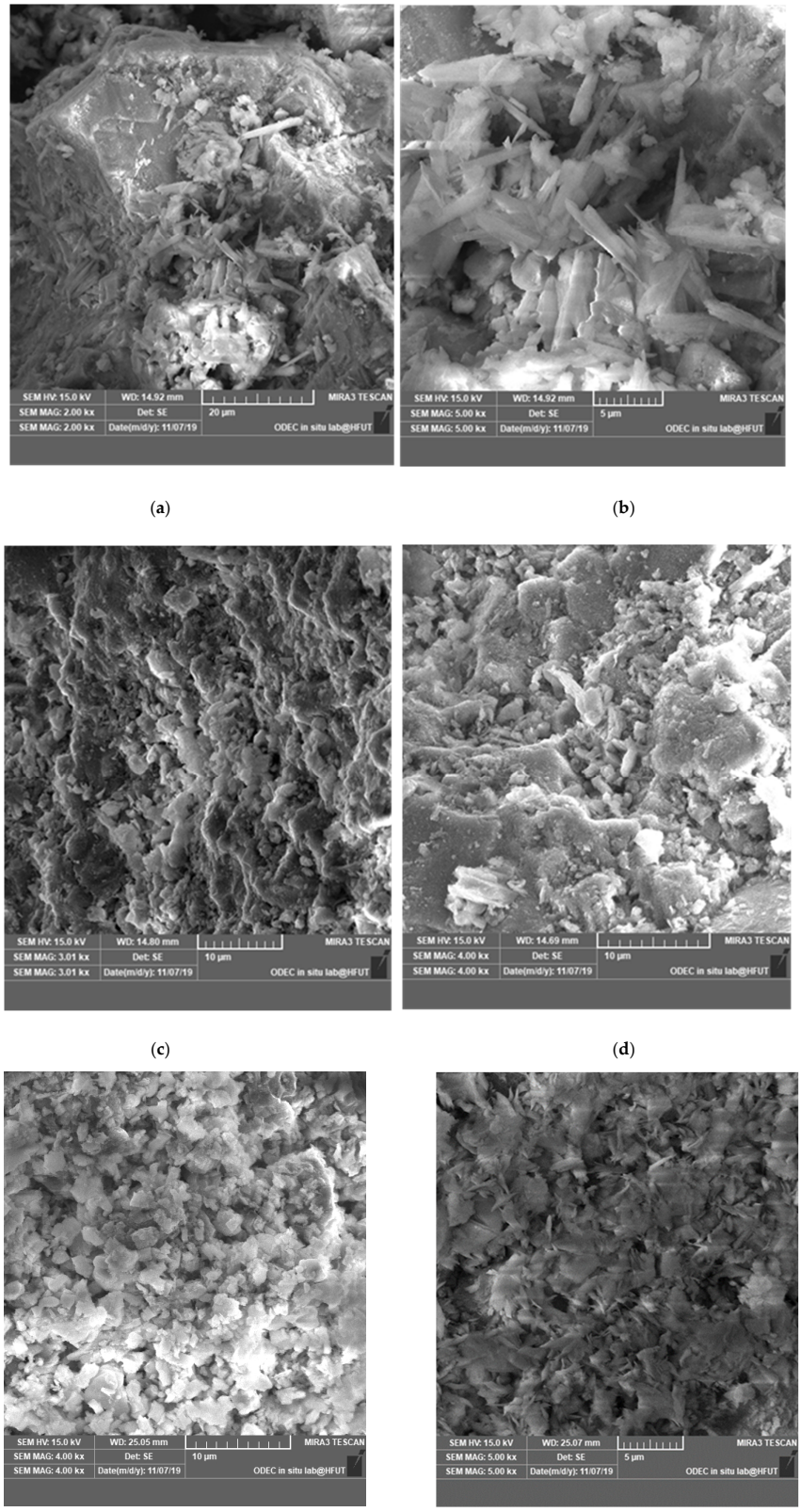


Figure 5. SEM images of A5 (**a**,**b**), B5 (**c**,**d**), and C3 (**e**,**f**). (**a**) Sample A5 magnified 2000 times; (**b**) Sample A5 magnified 5000 times; (**c**) Sample B5 magnified 3000 times; (**d**) Sample B5 magnified 4000 times; (**e**) Sample C5 magnified 4000 times; and (**f**) Sample C5 magnified 5000 times.

Figure 5a shows the A5 sample of solidified tailings enlarged by 2000 times. Spear, columnar, and massive minerals adhesions were bonded around the tailings, which could be identified as aragonite and calcite according to the XRD results. Figure 5b illustrates the A5 image sample of solidified tailings enlarged by 5000 times, in which the rod-shaped objects are approximately 2~3 μm in length and 0.5~1.5 μm in diameter at the top, which is similar to the shape of *Sarcocystis bassiana*. Figure 5c,d represent the B5 sample of solidified tailings enlarged by 3000 and 4000 times, respectively. Like Figure 5a,b, many spherical minerals and a small amount of massive minerals were cemented on the surface of the tailings sand particles. Figure 5e illustrates the A5 sample image of solidified tailings enlarged by 3000 times, in which more spherical and flocculent minerals are stacked and bonded together. Figure 5f clearly illustrates that numerous spherical and massive minerals are cemented with tailings.

4. Discussion

The above test results show that MICP technology can effectively improve the strength and stability of tailings and solidify heavy metal ions in tailings. Combined with the macro and micro test results, the mechanism of strength enhancement of tailings and the biochemical reaction mechanism of heavy metal ions in tailings are analyzed in detail.

4.1. The Mechanism of MICP Improve Strength

The average particle size (D50) of tailings sand is 0.28 mm, which can ensure the unimpeded transmission of microorganisms and nutrients [23,24]. This test adopts the method of injecting bacterial liquid first and then cementing liquid for grouting, with a total of eight times. In the process of MICP reaction, a large amount of $CaCO_3$ (aragonite/vaterite) was newly formed. Vaterite fills the gap of tailing sand and cements the loose tailing sand particles together, so as to improve the strength of tailing sand [4,25–27]. The effect improved with increasing bacterial concentration because: (1) the content of CO_3^{2-} produced by urease increased with increasing bacterial concentration; and (2) when the bacterial concentration was low, there was not enough vaterite to cement the loose tailings. The CS could provide urea and Ca^{2+}, but an excessively high concentration of the CS possibly inhibited the crystal structure of $CaCO_3$, which formed more calcite or aragonite and had side effects.

4.2. The Biochemical Reaction Mechanism of MICP Solidifying Heavy Metal Ions

From XRD and SEM results, it can be concluded that Cu, Zn, Mn, and Pb in the metal tailings were mainly fixed by MICP through coprecipitation and biosorption by bacteria. Based on the research on the solidification of a single heavy metal (Pb) by MICP, Jiang et al., (2019) [17] and Castro-Alonso et al., (2019) [28] explained the solidification mechanism both abiotically and biologically. The abiotic mechanism refers to the chemical reaction between the heavy metals and some elements in the bacterial or cementation solution to form precipitates, while the biological mechanism refers to the formation of cell-centered precipitates by urea hydrolysis. Based on the solidification mechanism, the hypothesis of multi-layer precipitation structure of various heavy metals was postulated and discussed. The bacterial solution was injected when metal tailings were solidified by MICP. As the pH of the bacterial solution was 9, the free Cu^{2+}, Zn^{2+}, Mn^{2+}, and Pb^{2+} in the tailings could form initial abiotic precipitation such as $Cu(OH)_2$, $Zn(OH)_2$, $Mn(OH)_2$, and $Pb(OH)_2$ under alkaline conditions, which is conducive to acid-base balance. When the cementation solution was added, urea began to hydrolyze, and the initial non-biological precipitation began to transform into biological precipitation, accompanied by other new precipitation. With an increase in the grouting time, $Cu(OH)_2$, $Zn(OH)_2$, $Mn(OH)_2$, and $Pb(OH)_2$ could be transformed into $CuCO_3$, $ZnCO_3$, $MnCO_3$, and $PbCO_3$, respectively. According to the XRD results, $Cu_2(OH)_2CO_3$ and MnO_2 were formed instead of $CuCO_3$ and

$MnCO_3$. In accordance with the previous experimental and the XRD results, we deduced that with the increase in bacterial concentration, the main precipitates were:

$$Cu_2(OH)_2CO_3 \Rightarrow MnO_2 \Rightarrow PbCO_3 \Rightarrow ZnCO_3 \Rightarrow CaCO_3 \text{ (Group A)}$$

$$Cu_2(OH)_2CO_3 \Rightarrow MnO_2 \Rightarrow ZnCO_3 \Rightarrow PbCO_3 \Rightarrow CaCO_3 \text{ (Group B)}$$

$$MnO_2 \Rightarrow Cu_2(OH)_2CO_3 \Rightarrow PbCO_3 \Rightarrow ZnCO_3 \Rightarrow CaCO_3 \text{ (Group C)}$$

As shown in Figure 6, bacteria are negatively charged and can attract positively charged heavy metal ions. The heavy metal ions were precipitated by MICP and wrapped in the outer layer of the bacteria, forming a biological multi-layer precipitation structure. According to the hypothesis diagrams, the innermost two layers were $Cu_2(OH)_2CO_3$ and MnO_2, and the outer two layers were $ZnCO_3$ and $PbCO_3$. Cu_2 $(OH)_2CO_3$ and MnO_2 were formed before the urea hydrolysis, while $ZnCO_3$ and $PbCO_3$ were continuously transformed with the urea hydrolysis. The reason that $Cu_2(OH)_2CO_3$ and MnO_2 did not transform into $CuCO_3$ and $MnCO_3$ could be the envelopment of $ZnCO_3$ and $PbCO_3$ in the outer layer, which prevented the transformation. Generally, $CaCO_3$ was first formed and wrapped in the outer layer of biological precipitation, and the outer layer of $CaCO_3$ could protect the inner layer of heavy metal precipitation from washing or acid dissolution. From the SEM images, we can see that there was considerable calcium carbonate precipitation in the surface layer, and there may be calcium carbonate in the inner layer of multilayer precipitation structure.

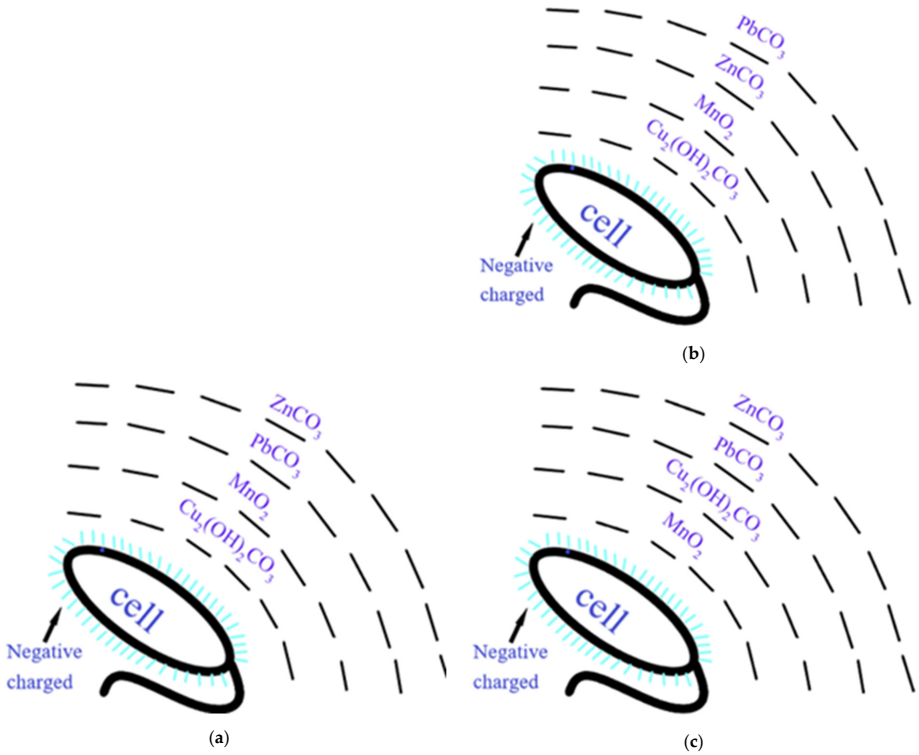


Figure 6. Layered precipitation structure hypothesis diagram. (**a**) Group A; (**b**) Group B; and (**c**) Group C.

5. Conclusions

(1) The bacterial and CS concentration were the two key factors of MICP. Within a certain range, there was a positive correlation between bacterial concentration and UCS. For CS, an excessively low concentration could not provide enough urea and calcium, while a high concentration could inhibit bacteria activity. Under experimental conditions, the optimal bacterial concentration OD600 was 1.6, and the optimal con-

centration of cementation solution was 1.0 mol/L. The corresponding compressive strength was 778 kPa;

(2) The concentrations of Cu^{2+}, Zn^{2+}, Mn^{2+}, and Pb^{2+} in the solidified tailings decreased during simulated leaching. Both bacterial concentration and cementation solution concentrations could affect the removal rate;

(3) The micro mechanism of MICP could be explained by abiotic and biological mechanisms. The hypothesis of the multi-layer precipitation structure of various heavy metals was first postulated and discussed in this study.

Author Contributions: Conceptualization, B.K. and F.Z.; methodology, H.L.; software, X.S.; validation, B.K. and L.X.; formal analysis, H.L.; investigation, Z.L.; resources, F.Z.; data curation, Z.L.; writing—original draft preparation, B.K.; writing—review and editing, B.K. and F.Z.; visualization, X.S.; supervision, F.Z.; project administration, F.Z.; funding acquisition, F.Z. All authors have readand agreed to the published version of the manuscript.

Funding: This research was funded by National Natural Science Foundation of China (grant numbers: 41877262, 42030710, 42107162), the National Natural Science Foundation of Anhui Province (grant number: 190885QD168), and the The Fundamental Research Funds for the Central Universities of China (grant number: PA2021 KCPY0055).

Institutional Review Board Statement: Not applicable.

Informed Consent Statement: Not applicable.

Data Availability Statement: Not applicable.

Acknowledgments: The authors express gratitude to the National Natural Science Foundation of China (Grant No. 41877262, 42030710, 41672306), Natural Science Foundation of Anhui Province (Grant No. 1908085QD168). The Fundamental Research Funds for the Central Universities of China (grant number: PA2021 KCPY0055).

Conflicts of Interest: The authors declare no conflict of interest.

References

1. Schmitt, C.J.; Whyte, J.J.; Roberts, A.P.; Annis, M.L.; May, T.W.; Tillitt, D.E. Biomarkers of metals exposure in fish from lead-zinc mining areas of Southeastern Missouri, USA. *Ecotoxicol. Environ. Saf.* **2007**, *67*, 31–47. [CrossRef] [PubMed]
2. Ternjej, I.; Srcek, V.G.; Mihaljevic, Z.; Kopjar, N. Cytotoxic and genotoxic effects of water and sediment samples from gypsum mining area in channel catfish ovary (CCO) cells. *Ecotoxicol. Environ. Saf.* **2013**, *98*, 119–127. [CrossRef] [PubMed]
3. Concas, A.; Ardau, C.; Cristini, A.; Zuddas, P.; Cao, G. Mobility of heavy metals from tailings to stream waters in a mining activity contaminated site. *Chemosphere* **2006**, *63*, 244–253. [CrossRef] [PubMed]
4. DeJong, J.T.; Fritzges, M.B.; Nusslein, K. Microbially induced cementation to control sand response to undrained shear. *J. Geotech. Geoenviron. Eng.* **2006**, *132*, 1381–1392. [CrossRef]
5. Cheng, L.; Cord-Ruwisch, R.; Shahin, M.A. Cementation of sand soil by microbially induced calcite precipitation at various degrees of saturation. *Can. Geotech. J.* **2013**, *50*, 81–90. [CrossRef]
6. Cheng, L.; Shahin, M.A.; Mujah, D. Influence of key environmental conditions on microbially induced cementation for soil stabilization. *J. Geotech. Geoenviron. Eng.* **2017**, *143*, 04016083. [CrossRef]
7. Wu, C.Z.; Chu, J. Biogrouting method for stronger bond strength for aggregates. *J. Geotech. Geoenviron. Eng.* **2020**, *146*, 06020021. [CrossRef]
8. Hu, X.S.; Liu, X.X.; Qiao, L.K.; Zhang, S.; Su, K.W.; Qiu, Z.L.; Li, X.H.; Zhao, Q.C.; Yu, C.H. Study on the spatial distribution of ureolytic microorganisms in farmland soil around tailings with different heavy metal pollution. *Sci. Total Environ.* **2021**, *775*, 144946. [CrossRef]
9. Tang, C.S.; Yin, L.Y.; Jiang, N.J.; Zhu, C.; Zeng, H.; Li, H.; Shi, B. Factors affecting the performance of microbial-induced carbonate precipitation (MICP) treated soil: A review. *Environ. Earth Sci.* **2020**, *79*, 94. [CrossRef]
10. Achal, V.; Pan, X.; Fu, Q.; Zhang, D. Biomineralization based remediation of As(III) contaminated soil by Sporosarcina ginsengisoli. *J. Hazard. Mater.* **2012**, *201–202*, 178–184. [CrossRef]
11. Jalilvand, N.; Akhgar, A.; Alikhani, H.A.; Rahmani, H.A.; Rejali, F. Removal of heavy metals zinc, lead, and cadmium by biomineralization of urease-producing bacteria isolated from iranian mine calcareous soils. *J. Soil Sci. Plant Nutr.* **2020**, *20*, 206–219. [CrossRef]
12. Wuana, R.A.; Okieimen, F.E. Heavy metals in contaminated soils: A review of sources, chemistry, risks and best available strategies for remediation. *ISRN Ecol.* **2011**, *2011*, 402647. [CrossRef]

13. Xu, D.C.; Zhou, P.; Zhan, J.; Gao, Y.; Dou, C.M.; Sun, Q.Y. Assessment of trace metal bioavailability in garden soils and health risks via consumption of vegetables in the vicinity of Tongling mining area, China. Ecotoxicol. *Environ. Saf.* **2013**, *90*, 103–111. [CrossRef] [PubMed]
14. Kang, C.H.; Han, S.H.; Shin, Y.J.; Oh, S.J.; So, J.S. Bioremediation of Cd by Microbially Induced Calcite Precipitation. *Appl. Biochem. Biotechnol.* **2014**, *172*, 2907–2915. [CrossRef] [PubMed]
15. He, Z.; Shentu, J.; Yang, X.; Baligar, V.C.; Zhang, T.; Stoffella, P.J. Heavy metal contamination of soils: Sources, indicators, and assessment. *J. Environ. Indic.* **2015**, *9*, 17–18.
16. Chen, X.; Guo, H.; Cheng, X. Experimental study of the improvement of the properties of the tailing by biomineralization. *Ind. Constr.* **2016**, *46*, 94–98, 176. (In Chinese)
17. Jiang, N.J.; Liu, R.; Du, Y.J.; Bi, Y.Z. Microbial induced carbonate precipitation for immobilizing Pb contaminants: Toxic effects on bacterial activity and immobilization efficiency. *Sci. Total Environ.* **2019**, *672*, 722–731. [CrossRef]
18. Peng, J.; Liu, Z. Influence of temperature on microbially induced calcium carbonate precipitation for soil treatment. *PLoS ONE* **2019**, *14*, e0218396.
19. Sun, X.; Miao, L.; Tong, T.; Wang, C. Study of the effect of temperature on microbially induced carbonate precipitation. *Acta Geotech.* **2019**, *14*, 627–638. [CrossRef]
20. Ramachandran, S.K.; Ramakrishnan, V.; Bang, S.S. Remediation of concrete using microorganisms. *ACI Mater.J.* **2001**, *98*, 3–9.
21. Gollapudi, U.K.; Knutson, C.L.; Bang, S.S.; Islam, M.R. A new method for controlling leaching through permeable channels. *Chemosphere* **1995**, *30*, 695–705. [CrossRef]
22. Oliveira, D.D.; Horn, E.J.; Randall, D.G. Copper mine tailings valorization using microbial induced calcium carbonate precipitation. *J. Environ. Manag.* **2021**, *298*, 113440. [CrossRef] [PubMed]
23. Xiao, P.; Liu, H.L.; Stuedlein, A.W.; Evans, T.M.; Xiao, Y. Effect of relative density and biocementation on cyclic response of calcareous sand. *Can. Geotech. J.* **2019**, *56*, 1849–1862. [CrossRef]
24. Zamani, A.; Montoya, B.M.; Gabr, M.A. Investigating challenges of in situ delivery of microbialinduced calcium carbonate precipitation (MICP) in fine-grain sands and silty sand. *Can. Geotech. J.* **2019**, *56*, 1889–1900. [CrossRef]
25. Chen, X.; Guo, H.; Cheng, X. Heavy metal immobilisation and particle cementation of tailings by biomineralisation. *J. Environ. Geotech.* **2018**, *5*, 107–113. [CrossRef]
26. Cardosoa, R.; Pedreirab, R.; Duartec, S.O.D.; Monteirod, G.A. About calcium carbonate precipitation on sand biocementation. *Eng. Geol.* **2020**, *271*, 105612. [CrossRef]
27. Liu, B.; Zhu, C.; Tang, C.S.; Xie, Y.H.; Yin, L.Y.; Cheng, Q.; Shi, B. Bio-remediation of desiccation cracking in clayey soils through microbially induced calcite precipitation (MICP). *Eng. Geol.* **2020**, *264*, 105389. [CrossRef]
28. Castro-Alonso, M.J.; Montañez-Hernandez, L.E.; Sanchez-Muñoz, M.A.; Macias Franco, M.R.; Narayanasamy, R.; Balagurusamy, N. Microbially Induced Calcium Carbonate Precipitation (MICP) and Its Potential in Bioconcrete: Microbiological and Molecular Concepts. *Front. Mater.* **2019**, *6*, 126. [CrossRef]